

Spatial and temporal variance of walleye pollock (*Theragra chalcogramma*) in the eastern Bering Sea

John K. Horne and Paul D. Walline

Abstract: Mobile acoustic surveys attempt to map and count aquatic organisms without biasing abundance estimates. Horizontal and vertical movements by target species may influence density measurements and net samples during acoustic surveys. To investigate the influence of fish movement on density data, we compared temporal and spatial variability of walleye pollock (*Theragra chalcogramma*) in three sets (2 night, 1 day) of 14.8-km transects in the eastern Bering Sea. Walleye pollock density distributions were also compared with those in the five nearest daytime survey transects. We found that horizontal density distributions did not change at temporal scales ≤ 4 h and that spatial variance remained consistent at scales ≤ 2.5 km. Spatial variance density patterns were similar in transects sampled during the day compared with those sampled at night and were also similar in along-shore compared with cross-shore transects. Transects that contained two biological scattering layers could be vertically separated into zooplankton and fish. Spatial variance patterns in the upper zooplankton layer mimicked those of passive tracers, while patterns in the lower layer were consistent with those previously observed for mobile nekton. Current sampling resolution of acoustic surveys adequately captures horizontal spatial variance of walleye pollock in the Bering Sea.

Résumé : Les inventaires acoustiques mobiles cherchent à cartographier et à dénombrer les organismes aquatiques sans fausser les estimations d'abondance. Les déplacements horizontaux et verticaux des espèces ciblées peuvent affecter les mesures de densité et fausser les échantillons nets durant l'inventaire. Afin d'évaluer l'influence des déplacements des poissons sur les données de densité, nous avons comparé la variation temporelle et spatiale chez des goberges de l'Alaska (*Theragra chalcogramma*) dans trois séries (2 de nuit et 1 de jour) de transects de 14,8 km dans l'est de la mer de Béring. Nous avons aussi comparé les répartitions de densité des goberges de l'Alaska à celles obtenues sur les cinq transects d'inventaires de jour les plus proches. Les répartitions horizontales de densité ne changent pas aux échelles temporelles de ≤ 4 h et la variance spatiale reste uniforme aux échelles de $\leq 2,5$ km. Les patrons de variance de la densité spatiale sont semblables sur les transects inventoriés le jour et la nuit, de même que chez ceux faits parallèlement et perpendiculairement à la rive. Dans les transects qui contiennent deux couches de diffusion biologique, nous pouvons distinguer verticalement le zooplancton et les poissons. Les patrons de variance spatiale de la couche supérieure de zooplancton imitent ceux de traceurs passifs, alors que les patrons de la couche inférieure concordent avec ceux observés antérieurement chez le nekton mobile. La résolution actuelle de l'échantillonnage des inventaires acoustiques permet de capter de façon adéquate la variance spatiale horizontale de la goberge de l'Alaska dans la mer de Béring.

[Traduit par la Rédaction]

Introduction

Characterizing the temporal and spatial behaviour of a target species is crucial to the successful census of aquatic nekton (Aglen 1994; Fréon and Misund 1999). Any movement by organisms during assessment surveys potentially biases density and subsequent abundance or biomass estimates. Remote sensing is one approach used to reduce bias

by increasing the proportion of the area or volume sampled and by increasing synopticity of a survey. Animal distribution patterns observed using remote sensors such as echosounders are dependent on the aperture of the sensor, the speed of the platform, the sampling rate of the instrument, the grouping of samples, and by organism movements relative to the sensor track. In aquatic surveys, vessel-mounted sensors with small apertures have a limited number of sur-

Received 29 October 2004. Accepted 29 June 2005. Published on the NRC Research Press Web site at <http://cjfas.nrc.ca> on 8 November 2005.
J18381

John K. Horne.¹ University of Washington, School of Aquatic and Fishery Sciences, Box 35520, Seattle, WA 98355, USA, and National Oceanic and Atmospheric Administration, National Marine Fisheries Service, Alaska Fisheries Science Center, 7600 Sand Point Way NE, Seattle, WA 98115, USA.

Paul D. Walline. National Oceanic and Atmospheric Administration, National Marine Fisheries Service, Alaska Fisheries Science Center, 7600 Sand Point Way NE, Seattle, WA 98115, USA.

¹Corresponding author (e-mail: jhorne@u.washington.edu).

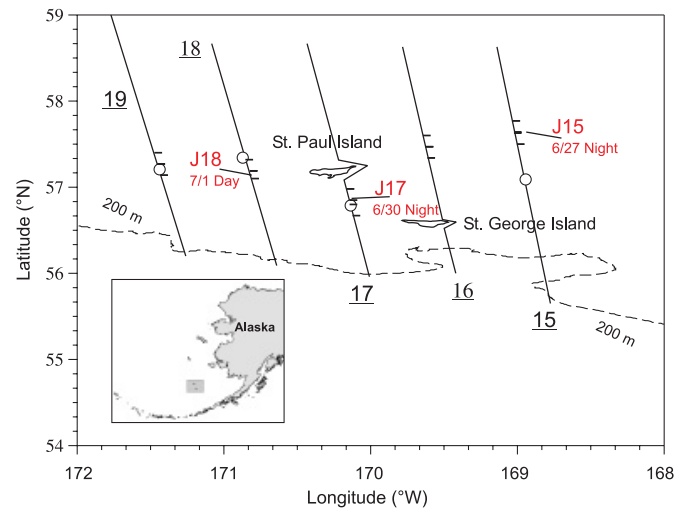
vey design variables that can be controlled by the user: temporal collection of data, spatial resolution of individual and grouped samples, and the spatial pattern of sampling.

A sampling spatial pattern, or survey design, is optimal if samples accurately characterize the abundance and distribution of a population while minimizing sampling effort. Since patchy distributions are a long-recognized trait of pelagic organisms (Hensen 1911; Hardy 1955; Steele 1976), survey designs must be sensitive to the spatial and temporal dynamics of the population being surveyed (Reid et al. 2000). Studies examining effects of dynamic fish distributions on accuracy of numeric or biomass estimates have traditionally focused on estimating uncertainty (e.g., Petitgas 2001; Gimona and Fernandes 2003) or bias of abundance estimates utilizing alternate sample layouts relative to population distributions (e.g., Simmonds and Fryer 1996; Kalikhman and Ostrovsky 1997). Less effort has focused on the effect of individual and aggregation movements relative to sampling resolution and on the potential confounding of animal movements with elapsed sampling time on abundance estimates. The challenge of designing an effective survey is further compounded when the geographic area of interest is large, the sampling speed is slow, and the sampling resolution of survey transects is coarse given the time constraints of a research vessel schedule.

Assessing adult biomass of walleye pollock (*Theragra chalcogramma*) in the eastern Bering Sea includes all of these challenges. Walleye pollock represents approximately 70% of the groundfish biomass in the eastern Bering Sea (Springer 1992). Commercial fishers took over six million metric tons a year in the late 1980s, but the catch has dropped to around three million metric tons in recent years (source: Food and Agriculture Organization of the United Nations (FAO) Fisheries Global Information System, <http://www.fao.org/fi/figis/index.jsp>). The highest catches represent up to 5% of the world's fish catch (Bailey et al. 1999). Walleye pollock are found throughout the middle and outer shelf domains of the eastern Bering Sea (Coachman 1986), necessitating a 300 000 km² survey area that extends from the Aleutian Island archipelago to the Russian–US border (e.g., Honkalehto et al. 2002). Acoustic surveys have assessed population numbers, biomass, and mapped summer distributions of walleye pollock on the continental shelf and slope at least every 3 years since 1979 (Traynor and Nelson 1985; Weststad 1993; Karp and Walters 1994). The survey is conducted over 2 months and typically logs a cruise track greater than 18 500 km (i.e., ~10 000 nautical miles, nmi). Since 1991, the cruise track has followed a boustrophedon sampling pattern, where regularly spaced, parallel transects are surveyed in alternating directions along a north–south axis.

Despite the ecological and commercial importance of commercial fish populations, such as walleye pollock, variability in density distributions at the sampling resolution of an acoustic survey (i.e., minimum 0.1-km horizontal integration bins and 10-km transect spacing) is not well described (Brodeur and Wilson 1996; Bailey et al. 1999). We were curious how observed distribution patterns may be confounded by the acoustic sampling resolution or by movement of fish during sampling. Walleye pollock were chosen as a representative species whose distributions and behaviors are typi-

Fig. 1. Location of midwater trawls (circles), full acoustic transects (numbers 15 through 19), extracted transects (tic marks on full transects), and repeated acoustic transects (J15, J17, and J18). The rectangle in the inset shows the location of the study transects within the Bering Sea.



cal of semidemersal and pelagic gadoids. A collection of repeated, extracted, and regular acoustic survey transects were used to quantify changes in walleye pollock density as a function of spatial scale and temporal sampling resolution.

Materials and methods

Data collection

An echo integration-trawl survey targeting walleye pollock was conducted on the eastern Bering Sea shelf between 7 June and 2 August 2000 aboard the National Oceanic and Atmospheric Administration (NOAA) ship *Miller Freeman* (see Honkalehto et al. 2002 for survey details). The survey consisted of 29 parallel transects spaced at 37 km (i.e., 20 nmi) and oriented north–south across the continental shelf (Fig. 1). Transect directions in the shelf survey are oriented approximately orthogonal to bathymetric contours and coincide with groundfish survey transects conducted by the same institution.

All regular transects were surveyed during daylight hours (~0500–2400 local time). On 27 June, 30 June, and 1 July, additional sets of 14.8 km (i.e., 8 nmi) transects, repeated four times, were surveyed orthogonal to the regular transects (i.e., east–west along shelf) (Table 1). Each of these short transects took approximately 1 h to complete. Two of the three repeated transect sets (J15 and J17) were conducted during dark hours, while the set on 1 July (J18) was completed during the day. All repeated transects were completed before sunrise or sunset to avoid vertical distribution changes associated with crepuscular periods. The location of repeated transects was determined using a combination of cruise logistics and presence of fish. Throughout the survey, fish were sampled using an Aleutian Wing Trawl (midwater) and an 83/112 eastern bottom trawl to identify species within aggregations or layers and to provide length frequency sam-

Table 1. Walleye pollock (*Theragra chalcogramma*) repeated transect data summary sampled in the eastern Bering Sea during June and July 2000.

Transect	Day (D) vs.		Start time	End time
	Night (N)			
J15a	N		0.3784722	0.41157407
J15b	N		0.4174769	0.45105324
J15c	N		0.4557986	0.48898148
J15d	N		0.4961921	0.53009259
J17a	N		0.3645949	0.39821759
J17b	N		0.4067477	0.44010417
J17c	N		0.4464699	0.47982639
J17d	N		0.4867361	0.52018519
J18a	D		0.1095602	0.14280093
J18b	D		0.1481481	0.18157407
J18c	D		0.1969213	0.23034722
J18d	D		0.2343056	0.26875000

Note: All times are Coordinated Universal Time (UTC). To convert to decimal hours, multiply UTC by 24.

Walleye pollock density was measured using a calibrated Simrad EK 500 splitbeam echosounder (Horten, Norway) operating at 38 kHz (Bodholt et al. 1989). All densities were recorded as nautical area scattering coefficients (s_A , $m^2 \cdot nmi^{-1}$). Acoustic data samples were filtered using an S_v threshold of -70 (dB re $1 m^{-1}$), inspected and corrected for bottom integration, vertically integrated from 14 m below the surface to 0.5 m above bottom, and binned at a horizontal distance of 185.2 m (i.e., 0.1 nmi). Since each of the repeated transects was 14.8 km in length, each transect data set contained 80 bins. To examine the potential presence of anisotropic density distributions, two additional 14.8-km sections of transect were extracted from the adjacent north–south survey transects and were binned in the same way. To increase the number of transects examined and to extend the range of the spatial variance analysis, the closest five full survey transects (transects 15–19) were also binned at 185.2-m resolution. Data from the full transects were vertically integrated from 14 m below the surface to 0.5 m or 1.0 m from the bottom (depending on bottom roughness and fish density). All echograms were scrutinized for species, and the analysis of fish was limited to walleye pollock. When plankton formed a layer near the surface, the top of the echo integration layer was lowered to 30 m below the surface. No mixing occurred between walleye pollock and the plankton layer during diel migrations.

Spatial analyses

Scale-dependent spatial variance of walleye pollock density distributions was characterized using spectral analysis (Jenkins and Watts 1968; Koopmans 1974; Chatfield 1984). The density data (i.e., s_A values) were first standardized by subtracting the mean and dividing by the standard deviation, a fast Fourier transform was applied to each set of s_A values, the results squared, and the periodogram smoothed using a triangular filter (Chatfield 1984). Least squares regression lines were fitted to log–log plots of spectral density and frequency. When a change in slope (i.e., an inflection point) was observed, the data were divided in two sections, and separate regression lines were fit to each section. Spectral

density values from replicate transects were averaged to facilitate comparison among sets at larger temporal scales.

Three additional metrics were used to examine similarity in the spatial scale-dependence of walleye pollock density distributions. One-dimensional variograms (using s_A values) were constructed for each transect, and then a model was fit by eye using EVA 2 software (Petitgas and LaFont 1997). The presence and characteristics of a nugget, sill, and range were described for each variogram model. Semivariance was also plotted as a function of distance between pairs of points (i.e., lag distance) in each transect. Lag units ranged from twice the horizontal resolution of the data (370 m) to half the distance of a repeated transect (7.4 km). In full transects, lag units started at 10 km. Correlograms were plotted for each transect, and autocorrelation radii were tabulated when the autocorrelation function approached zero (i.e., 0.003 or less).

Temporal analyses

To quantify temporal variability in one-dimensional, wall-eye pollock densities during 4-h sampling periods, changes in acoustic backscatter at each horizontal sampling bin (45 s) were tabulated as a function of time lag among bins within and among transect repetitions. A set of repeated transects consisted of four passes. There were a total of six possible pairs of time lags for each bin where a difference in density (Δs_A) and a difference in time (Δt) could be calculated. When Δs_A is plotted as a function of Δt , trends in density changes will be seen as deviations from $\Delta s_A = 0$.

Temporal changes in two-dimensional walleye pollock distributions were examined by comparing normalized density distributions between transect pairs within the 14.8-km repeated transect sets. Fish density similarity was investigated at the resolution of an acoustic cell (185 m horizontal by 5 m vertical) and summarized for each transect. The metric used is Syrjala's (1996) analog to a Cramér – von Mises test that compares the sum of squared differences between two cumulative distribution functions. Since the comparison metric is sensitive to the starting cell within a transect, the comparison was calculated starting at each corner of the transect. The final test statistic was an average of the four comparison values (Zimmerman 1993). The level of significance ($\alpha = 0.05$) of the test statistic was determined using a randomization test (Edgington 1980). Cells at corresponding locations in the two transects being compared were randomly assigned to one of the two transects. Densities were then tabulated in cumulative distribution functions for computation of the test statistic. One thousand randomizations were used to compute the empirical distribution function of the test statistic in each comparison. See Syrjala (1996) for additional details.

Results

Fish caught in midwater trawls closest to the repeated transect locations consisted of 35- to 55-cm walleye pollock (see trawl locations in Fig. 1). Some juvenile walleye pollock were caught in the midwater trawl on transect 15. Walleye pollock were vertically dispersed during the two nighttime, repeated-transect series (J15 and J17) and formed a layer between 50- and 75-m depth during the daytime se-

Table 2. Characteristics of walleye pollock (*Theragra chalcogramma*) spatial distribution in repeated, extracted, and regular acoustic transects surveyed in the eastern Bering Sea during summer 2000.

Series	Transect	s_A (m ² -nmi ⁻¹)	Autocorrelation radius (km)	Variogram			
				Nugget	Sill	Range (km)	
Repeated	J15a	351	—	Yes	No	Slight increase	
	J15b	198	0.4	Yes	No	Slight linear increase	
	J15c	278	3.3	Yes	No	Linear increase	
	J15d	221	2.8	Yes	No	Nonlinear increase	
	J17a	216	2.4	Yes	Yes	6.5	
	J17b	198	0.2	Yes	No	Slight linear increase	
	J17c	191	0.4	Yes	No	Pure nugget	
	J17d	212	0.6	Yes	Small	Almost pure nugget	
	J18a	1042	2.2	Yes	Small	~1.8, mostly nugget	
	J18b	947	5.6	Yes	No	Irregular increase	
	J18c	863	1.7	Yes	No	Slight linear increase	
	J18d	1002	2.4	Yes	No	Linear increase	
	Average		466	2.5			
	Extracted	15a	271	0.6	Yes	No	Pure nugget
15b		297	4.6	Yes	No	Nonlinear increase	
16a		2305	4.6	Small	No	Steep linear increase	
16b		1289	3.9	No	No	Steep linear increase	
17a		923	3.9	Yes	Yes	4.4	
17b		327	1.7	Yes	Yes	~1.8	
18a		1280	2.8	Yes	No	Linear increase	
18b		796	2.2	Yes	Yes	~3.0	
19a		291	3.9	Yes	No	Linear increase	
19b		334	2.2	Yes	Yes	<3.6	
Average			658	2.8			
Full	15	344	10.4	Yes	Yes	~37 (9.3)	
	16	1548	47.0	Yes	Yes	81.5 (11.1)	
	17	3025	53.3	Small	Yes	~88.9 (linear increase)	
	18	920	70.7	Yes	Yes	>55.6 (6.5)	
	19	907	79.8	Yes	Yes	>185.2 (linear increase)	
Average		1349	52.2				

Note: s_A denotes integrated water column acoustic backscatter (1 nmi = 1.852 km). Autocorrelation radius is the distance where the autocorrelation function reaches 0.003 or less. Experimental variograms are described using the presence or absence of a nugget and sill and a characterization of the range. For variograms without a sill, a description of the change in semivariance with lag distance is given. The information in parentheses (for the full transects) describes the model variogram fitted by eye when the maximum lag distance is restricted to the length of the repeated transects (14.8 km).

ries (J18). Near surface zooplankton layers were present during the J17 and J18 series. The upper 30 m of the water column was excluded from the analysis of fish spatial variance for all transects.

Fish densities were consistent within and among repeated transects (Table 2) but lower on average than those observed in the same area during the regular survey tracks (see extracted s_A values). Full survey transects had higher average s_A values than the repeated transects but also contained large sections with no fish. Repeated transects used in this analysis were not made in areas with high densities of walleye pollock.

Dominant spatial scales indicated by peaks in spectral density plots were difficult to visualize within histograms of acoustic fish density (Fig. 2; see also fig. 7.4 in Chatfield 1984). Spectral density values generally decreased from large to small scales, with fluctuating values at higher frequencies in all repeated transects. The peaks and troughs within spectral density plots at higher frequencies did not exactly coin-

cide among repeated transects (Fig. 3). Overall slopes of repeated transects were less than those observed at large scales (i.e., Steep in Table 3). Average transition scales (i.e., inflection points on the spectral density curves), interpreted as aggregation sizes of walleye pollock, were similar among the three repeated transect sets (J15: 2.4 km; J17: 2.8 km; J18: 2.3 km). Averaging spectral density values among repeated transects from each series resulted in smoothed average plots, but fluctuations remained at the higher frequencies (Fig. 3d). Average spectral density plots can be characterized by variable maximum values at the largest scale measured (14.8 km for the repeated transects), a continuous negative slope to a scale of approximately 1 km, and a reduced slope at scales less than 1 km.

Within regular survey transects, spectral density plots for walleye pollock differed from those for smaller targets assumed to be zooplankton (Fig. 4). Variance in zooplankton distributions exceeded those of walleye pollock at the largest scales measured. Zooplankton spectral densities decreased at

Fig. 2. Plot of walleye pollock (*Theragra chalcogramma*) density (s_A , $m^2 \cdot nmi^{-1}$) with distance along transect J18d (a) and resulting spectral density plot (b).

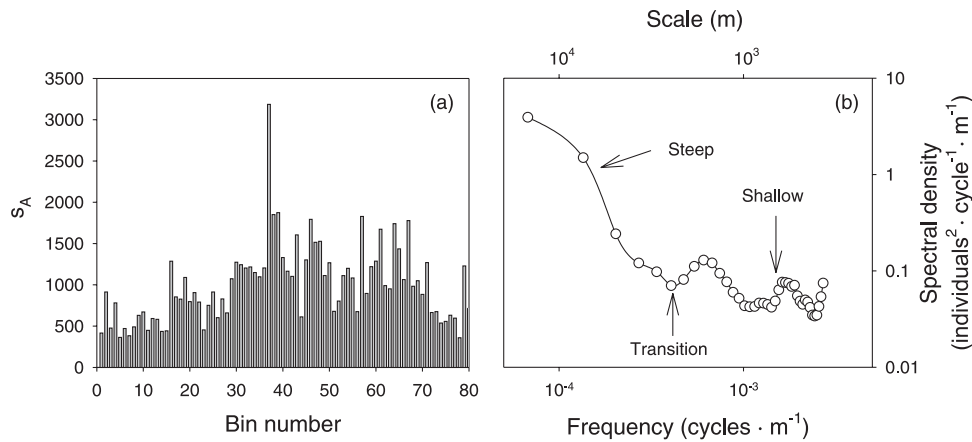
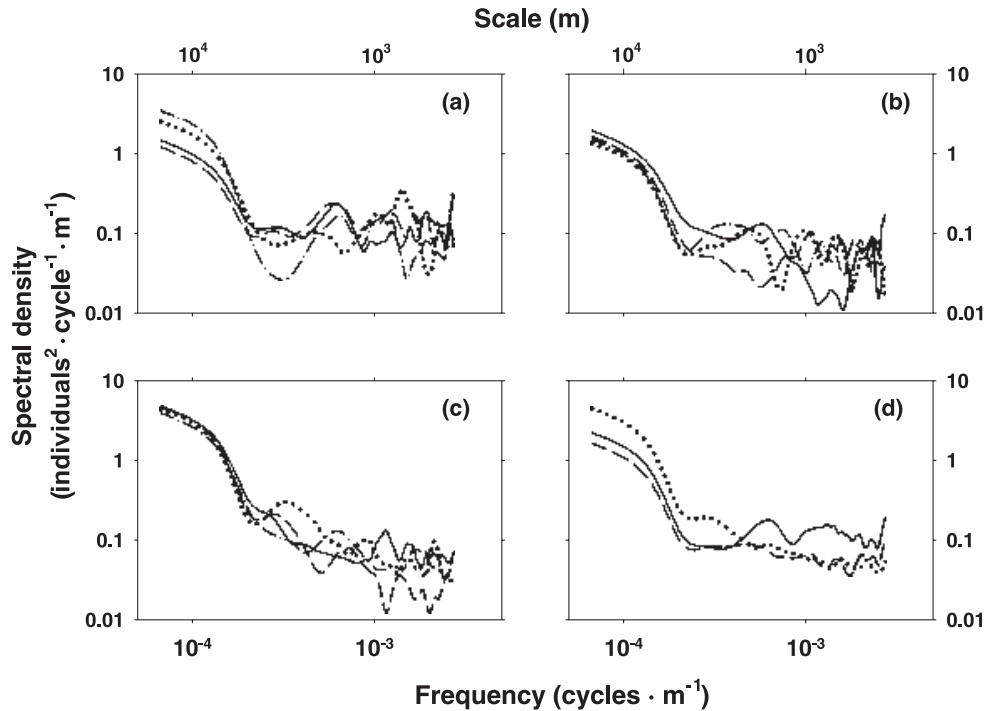


Fig. 3. Spectral density plots for repeated transect night series J15 (a) and J17 (b), repeated transect day series J18 (c), and the average of each series (d). For each series, the first repetition was drawn with a solid line, the second with a dashed line, the third with a dotted line, and the fourth with a dash-dotted line.



a relatively uniform rate over the entire range of scales examined. In contrast, walleye pollock spectral densities decreased at the largest scales and were nearly constant at scales ranging from a few kilometers to the minimum scale examined.

The averaged spectral density plot for series J18 was compared with the average spectral density plot from two 8 nmi sections of the adjacent transect 18. This comparison was used to examine the potential for anisotropic walleye pollock distributions during daylight hours. Differences in amplitudes and slopes of the spectral density plots from the north-south (18) and east-west transect series (J18) were slight (Fig. 5). No discernable trends were evident in the two plots,

suggesting that observed patterns in fish distributions are not influenced by acoustic transect orientation.

Variograms computed for the repeated transects showed no change or continuous increases in semivariance over the distance examined (7.4 km). Where no sill was evident, models fit to the data resulted in extrapolated ranges of tens to hundreds of kilometers. Variograms for the J15 transect series exhibited a temporal trend (Fig. 6). The variogram of transect J15a did not contain a sill and had a constant semivariance for lag distances of up to 7.4 km. The semivariance of transect J15b linearly increased from the smallest lag distance to a lag distance of 7.4 km. The semivariance of J15c and J15d increased linearly over the sampled range. Patterns

Table 3. Summary of spectral density plot slopes and transition scales for all transects.

Series	Transect	Overall	Steep	Shallow	Transition scale (km)	
Repeated	15a	-0.3	-1.7	0.1	2.1	
	15b	-0.3	-1.7	-0.25	2.5	
	15c	-0.4	-2.4	0	2.5	
	15d	-0.6	-3.3	-0.35	2.5	
	17a	-0.9	-1.9	-0.4	2.1	
	17b	-0.4	-2.1	0.3	1.6	
	17c	-0.6	-2.6	-0.3	3.7	
	17d	-0.5	-2.6	-0.2	3.7	
	18a	-0.8	-2.5	-0.1	2.5	
	18b	-1.2	-1.8	0.3	0.9	
	18c	-1	-2.7	-0.8	3.7	
	18d	-0.9	-2.4	-0.4	2.1	
	Extracted	15a	-0.6	-2.2	-0.4	3.7
		15b	-0.8	-2	-0.6	3
16a		-1.8	-1.8	-1.8	0	
16b		-1.8	-1.8	-1.8	0	
17a		-1.3	-1.3	-1.3	0	
17b		-1	-1	-1	0	
18a		-0.4	-1.9	0	3	
18b		-0.9	-2.3	-0.1	1.8	
19a		-0.7	-2.7	0.1	3	
19b		-0.8	-0.8	-0.8	0	
Full	15	-0.4	-0.4	-0.4	0	
	16	-1.3	-1.3	-1.3	0	
	17	-1.2	-1.3	5	0.5	
	18	-0.6	-1	0	0.8	
	19	-0.8	-0.8	1.4	0.5	

Note: Overall slope uses all points in the series, steep is the slope of the section prior to the transition, and shallow is the slope after the transition scale.

Fig. 4. Spectral density plot of the zooplankton layer (all s_A between 14 and 30 m) and that of walleye pollock (*Theragra chalcogramma*) (s_A deeper than 30 m) on transect 18.

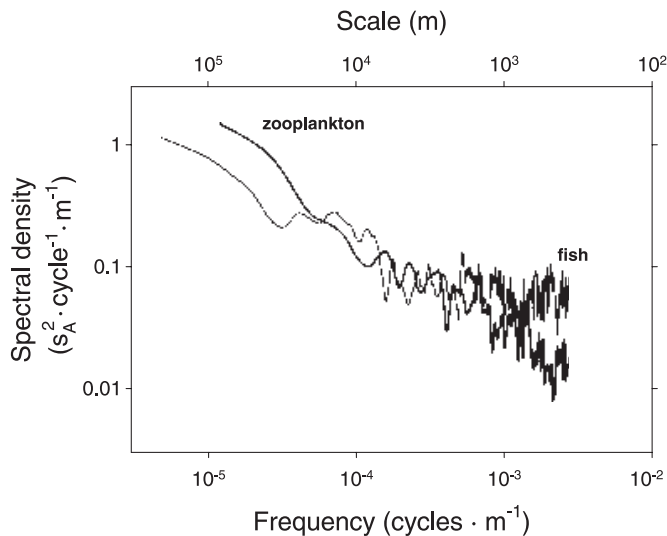


Fig. 5. Averaged spectral density plots from the short transect series J18 (solid line) and two extracted 8-nmi (1 nmi = 1.852 km) orthogonal daytime sections from transect 18 (dashed line).

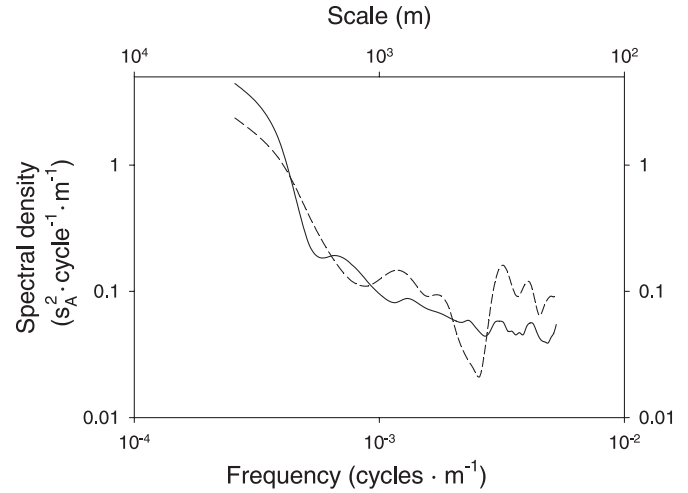
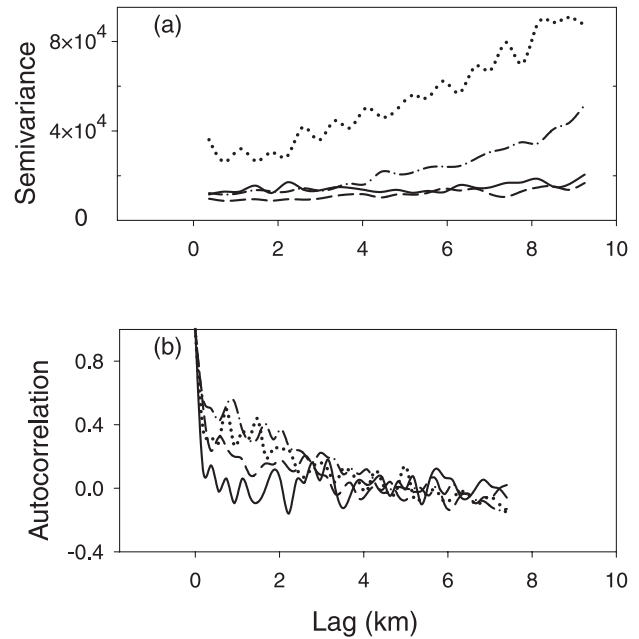
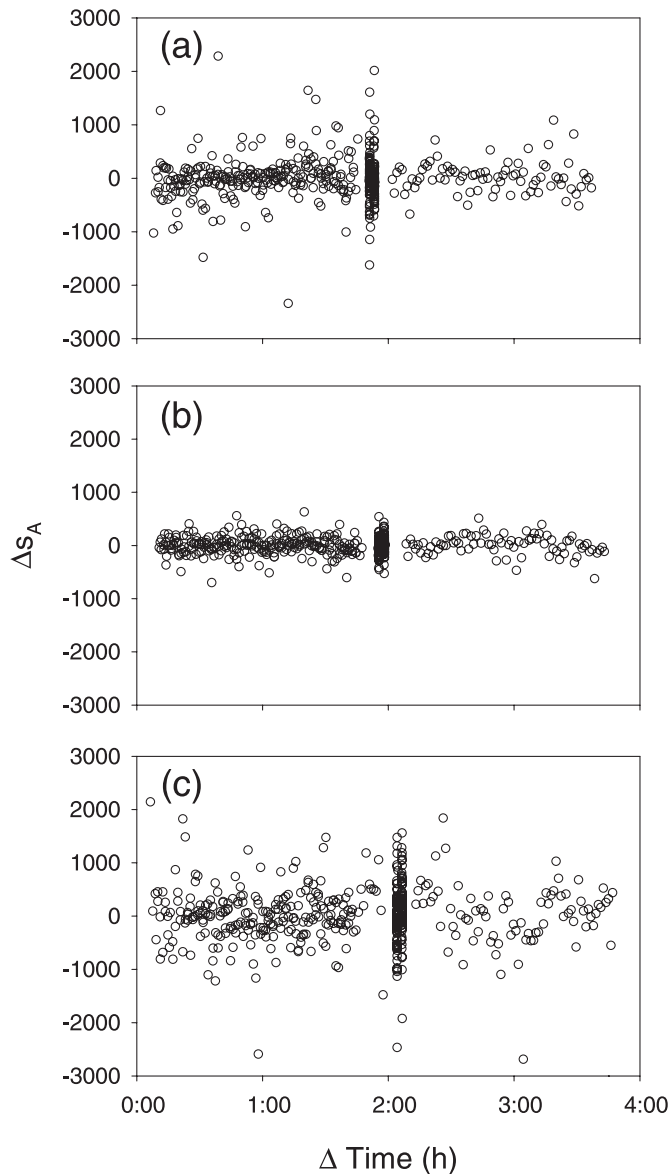


Fig. 6. Variograms (a) and correlograms (b) of transects J15a (solid), J15b (dashed), J15c (dotted), and J15d (dash-dotted).



observed in variograms of the extracted transects were consistent with those obtained from variography of full transects. In full transects surrounding the repeated transect sampling sites (i.e., transects 15 to 19), all but transect 18 had 56–93 km (i.e., 30–50 nmi) ranges despite poor behaviour in some experimental variograms. The variogram of transect 15 did not follow this trend. Transect 15 was characterized by a large nugget and erratic fluctuations of semivariance with lag distance. When the maximum lag distance in full transects was constrained to match the length of the repeated transects (i.e., 14.8 km), ranges in modeled variograms from full and repeated transects were directly comparable (see values in parentheses, Table 2). All constrained ranges in full

Fig. 7. Change in fish density (Δs_A) plotted as a function of lag time for each repeated transect series J15 (a), J17 (b), and J18 (c).



transects were larger than those observed in repeated transects.

As expected, results from autocorrelation analyses were comparable with those from one-dimensional variography. For all 14.8-km repeated and the extracted sections of complete transects, autocorrelation radii ranged from 0.1 to 5.6 km (Table 2). Autocorrelation radii for the set of complete transects averaged 52.2 km, an order of magnitude larger than the average of the repeated (2.5 km) or extracted (2.8 km) transects. When variograms exhibited nearly pure nugget behavior (e.g., J15a and J17b), the corresponding autocorrelation radii were short (Fig. 6).

Differences in walleye pollock integrated acoustic densities (i.e., s_A values) did not depend on the time difference between samples (Fig. 7). On average, s_A values remained constant at each location (i.e., 185-m horizontal bin) and did not increase as the time interval between any two samples increased. With the exception of five extreme values in the

Table 4. Comparison of walleye pollock (*Theragra chalcogramma*) density distributions (s_A , $m^2 \cdot nmi^{-1}$) within repeated 14.8-km (i.e., 8-nmi) transect sets using a modified Cramér – von Mises statistic (cf. Syrjala 1996).

Transect	a	b	c
15a	—	—	—
15b	0.0024 (0.601)	—	—
15c	0.0075 (0.098)	0.0031 (0.552)	—
15d	0.0269 (0.001)	0.0172 (0.018)	0.0088 (0.091)
17a	—	—	—
17b	0.0107 (0.087)	—	—
17c	0.0108 (0.081)	0.0232 (0.004)	—
17d	0.0100 (0.089)	0.0080 (0.151)	0.0107 (0.078)
18a	—	—	—
18b	0.0075 (0.014)	—	—
18c	0.0139 (0.001)	0.0056 (0.055)	—
18d	0.0201 (0.001)	0.0057 (0.108)	0.002 (0.486)

Note: p values are added in parentheses. Significant differences are in boldface.

J15 and J18 series, changes in acoustic densities were clustered close to zero for all sample time intervals.

Temporal similarity of two-dimensional walleye pollock density distributions differed among and within repeated transect sets (Table 4). Transect 15d differed from 15a and 15b in the first set. Transect 17b was different from 17c in the second set of repeated transects. In contrast, density distributions in transect 18a differed from all other repeated transects in the third transect set. A lower proportion of transects differed in transects sampled during dark hours (3/12) than those that were sampled during daylight hours (3/6) but only one day transect (18a) differed from the other three sampled during the day. No discernable trend was present in two-dimensional density differences between transect pairs as a function of time lag between or among repeated samples. The Cramér – von Mises test does not facilitate comparison among repeated transect sets.

Discussion

Techniques used to quantify variability in walleye pollock density distributions are applicable to many semidemersal or pelagic fish species and can be used in the design of mobile nekton acoustic sampling (Table 5). Spectral density curves from regular and repeated transect sets all contained slight negative slopes at small spatial scales. Observed near-constant variance at scales less than ~2 km means that horizontal bin sizes at or less than 2 km will include variability in walleye pollock density distributions. In contrast, the presence of steep and shallow slopes within spectral density plots of zooplankton layers from regular survey transects suggests that analytic cell sizes for mixed nektonic communities should be 200 m or less to characterize variation in zooplankton density distributions. The presence of steep and shallow slopes in spectral density plots of repeated and regular transects indicates that densities of walleye pollock aggregations were consistent at spatial scales equal to or less than ~2.5 km. The implication for survey sampling is that aggregation or school sizes are ~2.5 km in chord distance and that midwater or bottom trawl sampling used to verify

Table 5. Summary of analytic patterns observed, biological interpretation, and implication for acoustic abundance surveys.

Transect analytic pattern	Biological interpretation	Survey implication
Regular and repeated: slight negative slope at small scales	Constant small-scale variance	Scrutinizing resolution ≤ 1 nmi is fine
Regular: two layers with different spectral slopes		
Upper steeper than lower	Zooplankton, passive-like	To characterize zooplankton density distribution, must scrutinize ≤ 200 m
Lower small scale flatter	Fish, mobile	To characterize fish density distribution, must scrutinize ≤ 1 nmi
Repeated: two parts steep and shallow	Consistent density distributions at scales ≤ 2.5 km (patch size)	Patch size diameter ~ 2.5 km or 32 min at 2.5 knots for trawl sample
Alongshore vs. crossshore: break at same scale on both spectra; similar slopes on pairs of segments	Isotropic density distributions	Transect direction does not matter (should be checked for each species and season)
Day vs. night repeated: similar slopes and amplitudes within spectra	Density distributions are similar day and night	Sampling can be same day and night (should be checked for each species and season)
Temporal dependence: zero change in s_A as a function of time	No change in fish density distributions at temporal scales ≤ 4 h	Can return to spot for net sample within 4 h
Two-dimensional repeated: no consistent change with elapsed time	Fish density changing over small temporal scales	Difficult to catch specific fish
	Density changes horizontally and vertically	Should fish shortly after observation if want to sample a particular layer

Note: 1 nmi = 1.852 km.

species composition and to collect length frequency data must not exceed 32 min at a trawling speed of $1.3 \text{ m}\cdot\text{s}^{-1}$ (i.e., 2.5 knots) to remain within an observed aggregation. The similarity in spectral density plots from along-shore and cross-shore transects suggests isotropic density distributions of walleye pollock, and assuming that these samples are representative, the direction of transect sampling or trawling does not matter. Similarities in spectral density plots between day and night transects imply that variability in vertically integrated density distributions during summer months does not have a strong diel component and that transect layout and sampling can remain constant throughout a 24-hour period. If a significant portion of the target species occurs within the near-bottom dead zone, then biased density estimates may result. This observation is based on integrated water column backscatter using a limited number of samples and may not be consistent in other seasons, in depth-stratified samples, or for other fish species. Since changes in integrated water column fish densities were not dependent on elapsed time between acoustic measurements, changes in fish densities occurred at temporal scales ≤ 4 h. Therefore, representative species identification and length frequency samples can be obtained from a trawl sample as long as a location is fished within 4 h of the corresponding acoustic sample. It may be difficult to catch a specific school when trawling, but the net contents should be representative of individuals within an aggregation.

A variety of metrics can be used to characterize aggregation or patch sizes. The range parameter of a variogram is interpreted as the biological patch size (Rossi et al. 1992). The same interpretation is used for the autocorrelation radius (Legendre and Fortin 1989; Kalikhman and Ostrovsky 1997) and for slope changes in spectral density plots (Horne and Schneider 1997). In this study, estimates of walleye pollock

aggregation sizes differed depending on the metric used and, in part, on the length of the original transect. Extrapolated ranges from variogram models of full transects ranged between 37 and 185 km, autocorrelation radii were 2–3 km in length, and patch size inferred from changes in spectral density slopes averaged ~ 2.5 km. Inferred patch sizes were similar between autocorrelation radii and changes in spectral density slopes. Variogram ranges from full transects or calculated using restricted lag distances exceeded ranges of all other transects. Since the nugget contains measurement error and spatial variance at scales smaller than the lag unit, ranges smaller than the lag unit will not be detected. Increased lag distances used in calculating variograms for full transects are believed to contribute to the mismatch between ranges at small and large scales. Slopes of zooplankton and walleye pollock spectral density plots indicate that scale-dependent density distributions differed between the two groups. The shape and slope of the zooplankton spectral density plot is consistent with those of krill in the Southern Ocean (Weber et al. 1986; Levin et al. 1989), which mimic scale-dependent, spatial distribution patterns of passive tracers. The shallower slope of the walleye pollock spectral density plot is attributed to movement associated with aggregative behaviours (see also Horne and Schneider 1997).

The analytic techniques used in this study do have limitations. All three surface pattern techniques (Legendre and Fortin 1989) are based on estimates of lagged covariance functions: spectral analysis (Platt and Denman 1975), autocorrelation radii (Legendre and Fortin 1989), and variography (Rossi et al. 1992; Petitgas 1993). Lagged covariance techniques are sensitive to the presence of zero counts that may overestimate covariances (Fasham 1978; Legendre and Fortin 1989; Horne and Schneider 1997) and also sensitive to extreme values that may bias results (O'Driscoll et al.

2000). In our study, overall densities in repeated transects were low, but only 2 of 1760 cells within the 14.8-km transects contained zero s_A values. Wavelet analysis, an alternative to spectral analysis and variograms (Bradshaw and Spies 1992), can be used to investigate both local and global scale-dependent patterns but is typically used with nonstationary series (Hudgins et al. 1993; Lau and Weng 1995). The global wavelet spectrum has been shown to be equivalent to the true power spectrum (Percival 1995). We standardized all density series used in this study to ensure stationarity and focused the analysis on the global binning and timing of acoustic samples.

Temporal variability in walleye pollock densities differed depending on the observation scale and the number of dimensions used in the analysis. At temporal scales of 4 h or less and horizontal spatial scales of 185 m, acoustic backscatter values differed between some transect pairs in two spatial dimensions but not among cells when backscatter was integrated through the water column. This pattern was consistent within and among repeated transect sets, whether the sampling occurred during light or dark hours. The relation between sample unit size and spatial aggregation pattern has been shown to influence spatial variability (Sawyer 1989; Yamamura 1990) but additional effects due to flux (i.e., spatial movement over time) have received less attention (Gaston and McArdle 1994). A relevant resource management issue is the maintenance of population densities despite ongoing reductions in population abundances (cf. McArdle and Gaston 1993; Rose and Kulka 1999; O'Driscoll et al. 2000). Conflation of spatial with temporal variability has also been shown to systematically overestimate temporal variance in population abundance estimates (Stewart-Oaten et al. 1995).

Acoustic-based density measurements were not adversely affected by spatiotemporal movements of walleye pollock during summer months. Based on our samples, walleye pollock distributions appear to be isotropic, at least at spatial scales ranging from 185 m to 7.4 km (i.e., 0.1 to 4 nmi). The resulting acoustic density measurements and trawl samples were not dependent on the direction of sampling. Obviously, a single examination for the presence of anisotropy over a relatively short range of spatial and temporal scales is not definitive. Large-scale distributions should be detectable using the 37-km (i.e., 20-nmi) transect spacing currently used in Bering Sea surveys. Additional knowledge on the net flux of the population over the summer months, the degree of anisotropy over an increased scale range, and the association with strong depth or environmental gradients is required to eliminate potential sources of bias in walleye pollock abundance estimates. Empirical data collections on fish fluxes combined with computer simulations of alternate survey designs are recommended as the next step in this line of research.

Acknowledgements

We thank Dr. E. Loggerwell, Dr. S. Syrjala, Dr. R. O'Driscoll, and Mr. N. Williamson for reviews that clarified the manuscript. This study was supported by the Alaska Fisheries Science Center (NA17RJ1232-AM01) and the Office of Naval Research (N0014-00-1-0180).

References

- Aglen, A. 1994. Sources of error in acoustic estimation of fish abundance. *In* Marine fish behaviour in capture and abundance estimation. Edited by A. Fernö and S. Olsen. Fishing News Books, London. pp. 107–133.
- Bailey, K.M., Quinn, T.J., II, Bentzen, P., and Grant, W.S. 1999. Population structure and dynamics of walleye pollock, *Theragra chalcogramma*. *Adv. Mar. Biol.* **37**: 179–255.
- Bodholt, H., Nes, H., and Solli, H. 1989. A new echo sounder system. *Proc. Instit. Acoust.* **11**: 123–130.
- Bradshaw, G.A., and Spies, T.A. 1992. Characterizing canopy gap structure in forests using wavelet analysis. *J. Ecol.* **80**: 205–215.
- Brodeur, R.D., and Wilson, M.T. 1996. Mesoscale acoustic patterns of juvenile walleye pollock (*Theragra chalcogramma*) in the western Gulf of Alaska. *Can. J. Fish. Aquat. Sci.* **53**: 1951–1963.
- Chatfield, C. 1984. The analysis of time series: an introduction. Fourth edition. Chapman and Hall, London.
- Coachman, L.K. 1986. Circulation, water masses, and fluxes on the southeastern Bering Sea shelf. *Cont. Shelf Res.* **5**: 23–28.
- Edgington, E.S. 1980. Randomization tests. Second edition. Marcel Dekker, New York.
- Fasham, M.J. 1978. The application of some stochastic processes to the study of plankton patchiness. *In* Spatial pattern in plankton communities. Edited by J.H. Steele. Plenum Press, New York. pp. 131–156.
- Fréon, P., and Misund, O.A. 1999. Dynamics of pelagic fish distribution and behaviour. Fishing News Books, Oxford, UK.
- Gaston, K.J., and McArdle, B.H. 1994. Temporal variability of animal abundances. *Philos. Trans. R. Soc. Lond. B Biol. Sci.* **345**: 335–358.
- Gimona, A., and Fernandes, P.G. 2003. A conditional simulation of acoustic survey data: advantages and potential pitfalls. *Aquat. Living Resour.* **16**: 123–129.
- Hardy, A.C. 1955. A further example of the patchiness of plankton distribution. *Deep Sea Res. (Pap. Mar. Biol. Oceanogr.)* **3**(Suppl.): 7–11.
- Hensen, V. 1911. Das leben im ozean nach zahlungen seiner Bewohner. Übersicht und resultaten der quantitativen untersuchungen. *Ergebn. Plankton Expdn. derHumboldt Stiftung V.*
- Honkalehto, T., Williamson, N., Hanson, D., McKelvey, D., and de Blois, S. 2002. Results of the echo integration-trawl survey of walleye pollock (*Theragra chalcogramma*) conducted in the southeastern Bering Sea shelf and slope in June and July 2002. NOAA Fisheries, Alaska Fisheries Science Center, Seattle, Wash. AFSC Processed Rep.
- Horne, J.K., and Schneider, D.C. 1997. Spatial variance of mobile aquatic organisms: capelin and cod in Newfoundland coastal waters. *Philos. Trans. R. Soc. Lond. B Biol. Sci.* **352**: 633–642.
- Hudgins, L., Friehe, C.A., and Mayer, M.E. 1993. Wavelet transforms and atmospheric turbulence. *Phys. Rev. Lett.* **71**: 3279–3282.
- Jenkins, G.M., and Watts, D.G. 1968. Spectral analysis and its applications. Holden-Day, San Francisco.
- Kalikhman I., and Ostrovsky, I. 1997. Patchy distribution fields: survey design and adequacy of reconstruction. *ICES J. Mar. Sci.* **54**: 809–818.
- Karp, W.A., and Walters, G.E. 1994. Survey assessment of semi-pelagic gadoids: the example of walleye pollock, *Theragra chalcogramma*, in the eastern Bering Sea. *Mar. Fish. Rev.* **56**: 8–22.
- Koopmans, L.H. 1974. The spectral analysis of time series. Academic Press, New York.
- Lau, L.-M., and Weng, H. 1995. Climate signal detection using wavelet transform: how to make a time series sing. *Bull. Am. Meteorol. Soc.* **76**: 2391–2402.

- Legendre, P., and Fortin, M.J. 1989. Spatial pattern and ecological analysis. *Vegetatio*, **80**: 107–138.
- Levin, S.A., Morin, A., and Powell, T.M. 1989. Patterns and processes in the distribution and dynamics of Antarctic krill. Scientific Committee for the Conservation of Antarctic Marine Living Resources (SC-CAMLR)-VII/BG/20. pp. 281–296.
- McArdle, B.H., and Gaston, K.J. 1993. The temporal variability of populations. *Oikos*, **67**: 187–191.
- O'Driscoll, R.L., Schneider, D.C., Rose, G.A., and Lilly, G.R. 2000. Potential contact statistics for measuring scale-dependent spatial pattern and association: an example of northern cod (*Gadus morhua*) and capelin (*Mallotus villosus*). *Can. J. Fish. Aquat. Sci.* **57**: 1355–1368.
- Percival, D.P. 1995. On estimation of the wavelet variance. *Biometrika*, **82**: 619–677.
- Petitgas, P. 1993. Geostatistics for fish stock assessments: a review and an acoustic application. *ICES J. Mar. Sci.* **50**: 285–298.
- Petitgas, P. 2001. Geostatistics in fisheries survey design and stock assessment: models, variances and applications. *Fish. Fish.* **2**: 231–249.
- Petitgas, P., and Lafont, T. 1997. Eva2: estimation of variance version 2. A geostatistical package on Windows 95 for estimating precision of fish stock assessment surveys. *ICES CM 1997/Y 22*.
- Platt, T., and Denman, K.L. 1975. Spectral analysis in ecology. *Annu. Rev. Ecol. Syst.* **6**: 189–210.
- Reid, D., Scalabrin, C., Petitgas, P., Masse, J., Aukland, R., Carrera, P., and Georgakarakos, S. 2000. Standard protocols for the analysis of school based data from echo sounder surveys. *Fish. Res.* **47**: 125–136.
- Rose, G.A., and Kulka, D.W. 1999. Hyperaggregation of fish and fisheries: how catch-per-unit-effort increased as the northern cod (*Gadus morhua*) declined. *Can. J. Fish. Aquat. Sci.* **56**(Suppl. 1): 118–127.
- Rossi, R.E., Mulla, D.J., Journel, A.G., and Franz, E.H. 1992. Geostatistical tools for modeling and interpreting ecological spatial dependence. *Ecol. Monogr.* **62**: 277–314.
- Sawyer, A.J. 1989. Inconstancy of Taylor's b: simulated sampling with different quadrat sizes and spatial distributions. *Res. Popul. Ecol.* **31**: 11–24.
- Simmonds, E.J., and Fryer, R.J. 1996. Which are better, random or systematic acoustic surveys? A simulation using North Sea herring as an example. *ICES J. Mar. Sci.* **53**: 39–50.
- Springer, A. 1992. A review: walleye pollock in the North Pacific — how much difference do they really make? *Fish. Oceanogr.* **1**: 80–96.
- Steele, J.H. 1976. Patchiness. *In*. The ecology of the seas. *Edited by* D.H. Cushing and J.J. Walsh. Blackwell Scientific Publications, London. pp. 98–115.
- Stewart-Oaten, A., Murdoch, W.W., and Walde, S.J. 1995. Estimation of temporal variability in populations. *Am. Nat.* **146**: 519–535.
- Syrjala, S.E. 1996. A statistical test for a difference between the spatial distributions of two populations. *Ecology*, **77**: 75–80.
- Traynor, J.J., and Nelson, M.O. 1985. Results of the U.S. hydro-acoustic survey of pollock on the continental shelf and slope. *Int. North Pac. Fish. Comm. Gull.* **44**: 192–199.
- Weber, L.H., El-Sayed, S.Z., and Hampton, I. 1986. The variance spectra of phytoplankton, krill and water temperature in the Antarctic Ocean south of Africa. *Deep-Sea Res.* **33**: 1327–1343.
- Wespestad, V.G. 1993. The status of Bering Sea pollock and the effect of the "Donut Hole" fishery. *Fisheries*, **18**: 18–24.
- Yamamura, K. 1990. Sampling scale dependence of Taylor's power law. *Oikos*, **59**: 121–125.
- Zimmerman, D.L. 1993. A bivariate Cramér-von Mises type of test for spatial randomness. *Appl. Stat.* **42**: 43–54.